This is a non-peer reviewed preprint submitted to EarthArXiv.
The manuscript has been submitted for review in Environmental Research Letters.

Archetypal flow regime change classes as signatures of anthropogenic drivers of global streamflow alterations

Vili Virkki[1,2,*], Reetik Kumar Sahu[2], Mikhail Smilovic[2], Josias Láng-Ritter[1,3], Miina Porkka[1,4], Matti Kummu[1,*]

[1] Water and Development Research Group, Aalto University; Espoo, Finland
[2] Water Security Research Group, Biodiversity and Natural Resources Program, International Institute for Applied Systems Analysis (IIASA); Laxenburg, A-2361, Austria
[3] GIScience for Sustainability Transitions Lab, Aalto University; Espoo, Finland
[4] Department of Environmental and Biological Sciences, University of Eastern Finland; Joensuu, Finland

* Corresponding authors. Email: vili.virkki@aalto.fi, matti.kummu@aalto.fi

Abstract

Streamflow – a key component of the water cycle – is experiencing drastic alteration due to human actions. While existing studies have widely assessed the global extent and degree of this change, understanding of its drivers has been limited because previous global-scale approaches have largely relied on modelled hypothetical scenarios. Here, we overcome these limitations by providing a systematic association analysis of streamflow change and its drivers. We use observed streamflow data in 5,163 catchments globally and combine them with data on precipitation, evapotranspiration, water use, and damming. Building on a robust annual trend analysis covering years 1971–2010, we first determine archetypal flow regime change (FRC) classes, and then use them to investigate associations between streamflow change and its drivers. We find that 89% of all catchments are assigned to four main FRCs, which indicates globally consistent flow regime changes. By associating driver trends with the FRCs, we further characterise them by trends and changes in the four investigated drivers. We find that FRCs depicting decreasing streamflow quantity and variability are strongly associated with direct human drivers, either from water use or damming. In contrast, indirect drivers (precipitation and evapotranspiration) are more dominant in FRCs that depict increasing streamflow quantity and variability. Our observation-based association analysis substantiates the findings of existing model-based studies and can thus add detail and validation to their interpretations. This may support developing and adopting efficient measures to mitigate streamflow change and its subsequent impacts across scales.

1. Introduction

The global freshwater cycle has undergone drastic, anthropogenically driven changes since industrialisation. Globally widespread streamflow alterations are perhaps some of the most prominent examples of this change (Gudmundsson et al., 2021; Virkki et al., 2022; Yang et al., 2021). These alterations have become so pervasive that recent studies have suggested they undermine the Earth system functions related to freshwater and elevate risks related to diminishing resilience and stability of the Earth system (Gleeson et al., 2020; Porkka et al., 2024; Richardson et al., 2023). To effectively mitigate these risks, it is important to disentangle the underlying drivers behind the remarkable global change in streamflow.

The key drivers of streamflow alteration are related to climatic factors modifying water availability and human actions on the land surface diverting the flows of this water. Climate change and variability alter the spatiotemporal distribution of precipitation and evapotranspiration (Adler et al., 2017; Zhang et al., 2023), and land cover change can further attenuate or amplify these impacts by modifying the land-atmosphere moisture exchange (Theeuwen et al., 2023; Wang-Erlandsson et al., 2018). These indirect drivers affect runoff generation and, ultimately, streamflow volume. Once streamflow is generated from the available water, it may be altered by direct human actions. Consumptive water use, mainly for agricultural purposes, may appropriate and divert streamflow from its natural course (Huang et al., 2018; Wada and Bierkens, 2014), and flow regulation by dams and reservoirs may change the temporal distribution of streamflow, often towards homogenised flow regimes (Best, 2019; Grill et al., 2019; Poff et al., 2007).

Studies across scales have assessed the contributions of different drivers on streamflow alterations. Yet, global-scale studies often lack the depth and detail of local and regional approaches that can, for instance, incorporate highly specialised hydrological modelling setups and extensive data (Dennedy-Frank and Gorelick, 2019; Horton et al., 2021) or advanced empirical models (Chagas et al., 2022; Levy et al., 2018). Global studies on streamflow change often focus on describing the hydrological outcome and attaching driver attribution to this by, for example, qualitative discussion (Porkka et al., 2024), static information on human drivers (Yang et al., 2021), or incorporation of a limited set of drivers (Zhang et al., 2023). In studies whose main objective is explicit driver attribution, perhaps the most prominent approach at the global scale is to utilise hydrological modelling scenarios with variable driver configurations (Gudmundsson et al., 2021; Kåresdotter et al., 2022; Pastor et al., 2022; Veldkamp et al., 2018). This general approach is based on running globally applicable hydrological models in a suite of scenarios, including or excluding one or more drivers at a time. Model outputs are then compared to assess how much each inclusion or exclusion affects modelled streamflow, and the differences between scenarios are attributed to the distinct drivers.

The above approach, however, suffers from two major drawbacks. First, global hydrological models can strictly assess the hydrological impacts of mechanisms and interactions implemented in the models, which are relatively simplified with variable parameterisations and uncertainties (Telteu et al., 2021). Second, the assessed scenarios

are largely hypothetical – for instance, a typical control scenario in global hydrological modelling may assume static climate and dynamic water use (Frieler et al., 2024). These scenarios, thus, do not necessarily represent hydrological systems that have existed in the past, which further deepens the dependence on how these systems are mechanistically implemented in the models. We therefore argue that the hypothetically based global approaches leave room for improvement and validation in assessing the drivers of streamflow change at the global scale. This is especially relevant because the direct and indirect drivers depend on each other, and streamflow changes have been observed more commonly in catchments that are influenced by both types of drivers (Yang et al., 2021).

This study overcomes the limitations of existing global-scale driver attribution studies by composing a near-global, observation-based association analysis of streamflow change and its drivers. We present an annual trend analysis covering years 1971–2010, utilising streamflow observations and global data on four drivers: precipitation, evapotranspiration, water use, and damming. Our large sample of catchments with streamflow observations across the globe allows for robustly associating common streamflow regime alterations with their drivers. Moreover, our approach to spatially correlate observed streamflow trends with driver trends is less assumptive and dependent on modelling scenarios than existing global-scale approaches. Therefore, our approach is balanced between using historically coherent evidence and a large enough sample size to observe global patterns of streamflow change and its alignment with related drivers.

2. Methods

Fig. 1 presents the methodological outline of this study. To compose a global sample of streamflow data, we queried the Global Streamflow Indices and Metadata Archive (GSIM) (Do et al., 2018; Gudmundsson et al., 2018) to find catchments with a sufficiently long and reliable monthly streamflow record. We determined flow regime change (FRC) classes that depict archetypal streamflow regime alteration based on linear trends in four annual streamflow metrics. We similarly derived linear trends in the indirect and direct drivers using 0.1-degree resolution monthly precipitation and evapotranspiration data from ERA5-Land (Muñoz-Sabater et al., 2021), 0.5-degree resolution monthly total consumptive water use data from Huang et al. (2018), and dam records from GeoDAR (Wang et al., 2022). Finally, we grouped driver trends using four main FRC classes to reveal how streamflow change and its drivers are associated.

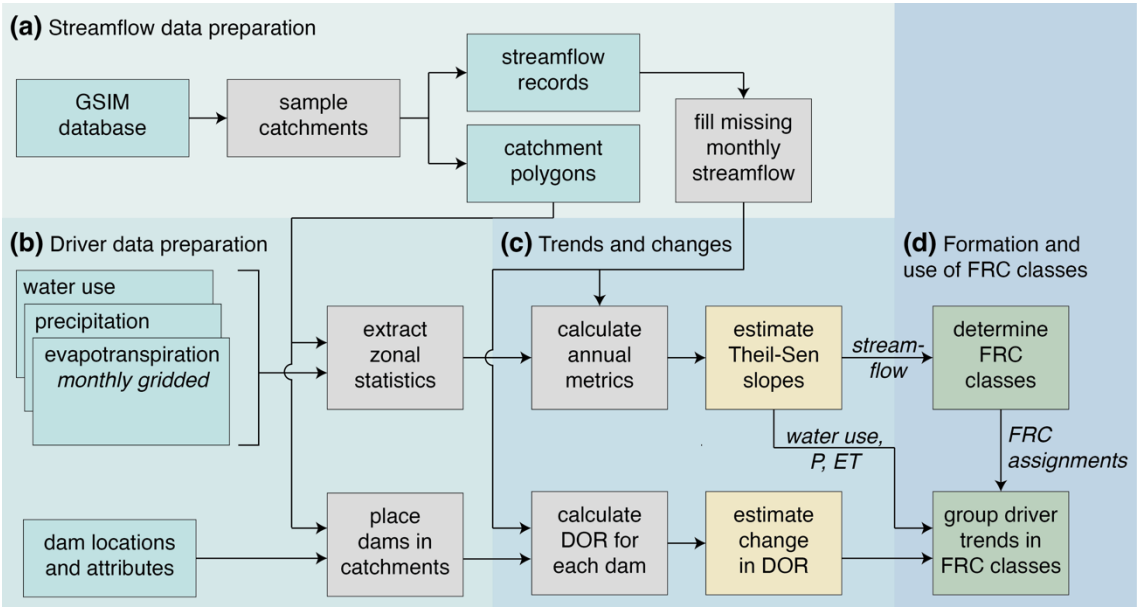

Figure 1. Methodological outline of the study. Streamflow data were prepared by sampling catchments and filling in missing monthly data entries (a). Driver data were prepared by extracting zonal statistics (for precipitation; P, evapotranspiration; ET, and water use) and querying dam points within catchment polygons (b). Monthly values were then transformed into annual metrics, followed by an assessment of linear trends using Theil-Sen slopes (streamflow, P, ET, water use) and absolute change in the degree of regulation (DOR) for dams (c). Finally, trends in four streamflow metrics were used to assign catchments to flow regime change (FRC) classes that were subsequently used to group driver trends and changes to associate streamflow change with its drivers (d).

2.1. Data preparation

The GSIM database collates streamflow observations from national authorities and international collections, covering over 35,000 streamflow records in a consistently formatted and quality-controlled collection (Do et al., 2018; Gudmundsson et al., 2018). Out of these, we selected all mean monthly streamflow records that fulfilled three conditions: 1) the catchment area is greater than 1,000 km^2; 2) streamflow observations cover at least ten years within 1971–2010; and 3) more than 50% of monthly values between the first and last month of record are available. Although streamflow data were available before 1971 and after 2010, the temporal extent was limited by the driver data availability on water use. Missing monthly streamflow values were filled with the mean of available values of the same month within ±10 years of the missing value. These conditions ensured that the selected catchments were large enough for zonal statistics and that the streamflow records were long enough for fitting linear trends.

To ensure accuracy for zonal statistics, streamflow records flagged as 'caution' were mainly discarded. This GSIM quality flag is marked for records whose delineated catchment area differs from the reported catchment area by more than 50% and for records with no reported catchment area. However, we included 415 records with no reported catchment area in GSIM. This was done by matching the streamflow gauge station and river names with a newer release of the GRDC station catalogue (GRDC, 2023) and assessing that the delineated GSIM catchment area had a less than 50% mismatch with the matched GRDC reported catchment area. Duplicate catchments were additionally handled by identifying catchment groups in which all catchments had more

than 90% area overlap with each other. In the identified duplicate groups, the catchment with the longest streamflow record was selected, totalling 513 preserved duplicates; 602 redundant duplicates were discarded.

After applying the above sampling criteria, 5,163 catchment records from GSIM were included, with 4,296 catchments having at least 20 years and 3,292 catchments having at least 30 years of record (Fig. S1a). A majority (76%) of all streamflow records had more than 90% of monthly mean streamflow values available (Fig. S1b). All continents were represented in the selected records; however, most catchments (82%) were in Europe, North America, or South America.

For monthly gridded precipitation, evapotranspiration, and total water use data, we extracted zonal statistics within catchment boundaries provided by GSIM. The time period for which zonal statistics were extracted equalled the streamflow record in each catchment. As all three variables were expressed as water column depths (millimetres/month), we used cell area-weighted mean as the aggregation metric, utilising the *exact_extract* R function (Baston, 2022). This function considers partial overlaps between polygon and gridded data, using in summarisation only the fraction of each grid cell that overlaps with the catchment boundary. While this increases the utility of zonal statistics for small catchments and coarse driver data, it also assumes that the respective grid variable value is spread evenly over the grid cell, incurring some uncertainty.

The GeoDAR database georeferences approximately 25,000 dam records from the World Register of Dams (WRD) and is currently the most comprehensive global database containing both locations and attributes of large dams (Wang et al., 2022). Although dam locations are openly available in GeoDAR, dam attributes are proprietary to the WRD. We updated the dam attributes with recent data from the WRD (retrieved on 20 July 2023). Dams within each catchment boundary were queried by point-in-polygon operations, and the reservoir capacity of each matched dam was related to the total annual volumetric streamflow at the catchment outlet. This corresponds to the commonly used metric 'degree of regulation' (DOR) (Nilsson et al., 2005). We set the DOR value of each dam to apply from the first month of the year of dam completion, and cumulatively summed the DOR values for each catchment. The cumulative DOR only considered increasing regulation as removed dams are absent in the WRD.

2.2. Trend analysis and flow regime change (FRC) classification

Throughout the analysis, we estimated linear trends using Theil-Sen regression, which is a robust linear regression method that outputs the median of trend slopes between all possible pairs of data points (Hurtado, 2020). This makes the resulting Theil-Sen slope less sensitive to outliers, which could be caused by the filled missing values, for instance. We estimated Theil-Sen slopes using annual metrics, which were computed from monthly streamflow and driver values (except for DOR). For streamflow, we calculated annual metrics and subsequently estimated trends for annual mean, standard deviation, and 5^{th} and 95^{th} percentiles. For precipitation and evapotranspiration, we used annual mean and standard deviation, whereas for water use, we used annual mean only.

Each catchment was assigned an FRC class based on the Theil-Sen slopes of four annual streamflow metrics (Table 1; Fig. S2). Four main FRCs were predefined: decreasing and increasing trends in mean streamflow (depicting quantity) characterised the 'shift down' and 'shift up' FRCs, respectively, whereas decreasing and increasing trends in the standard deviation of streamflow (depicting variability) characterised the 'shrink' and 'expand' FRCs, respectively. Conditions on trend direction were not enforced for one of the four streamflow trends in each FRC (labelled 'unconstrained' in Table 1). The four main FRCs thus comprised eight out of sixteen possible combinations that can be derived from trend directions in four streamflow metrics. Catchments with one of the remaining eight trend combinations not covered by the four main FRCs were assigned a class 'other'. This was also done for special cases where the Theil-Sen slope was zero, for instance, when the 5th percentile streamflow was zero throughout the record.

Table 1. Assignment rules for the four main flow regime change (FRC) classes. For each catchment and streamflow metric (mean, standard deviation, high flow, low flow), trends (Theil-Sen slopes) were computed based on annual metrics within the interval 1971–2010, with the sample size ranging from 10 to 40 years, depending on streamflow record length in each catchment (Fig. S1). Catchments were assigned to an FRC class based on the combination of four Theil-Sen slopes; in the Table, 'decreasing' means that the Theil-Sen slope is negative, and 'increasing' means that the Theil-Sen slope is positive. For conditions marked as 'unconstrained', the Theil-Sen slope can be either negative or positive. Should the combination of four trends in a catchment not match any of the four main FRC classes, it was assigned a class 'other'.

Streamflow metric	*Flow regime change (FRC) class*			
	'shift down'	**'shift up'**	**'shrink'**	**'expand'**
mean	decreasing	increasing	unconstrained	unconstrained
standard deviation	unconstrained	unconstrained	decreasing	increasing
high (95th percentile) flow	decreasing	increasing	decreasing	increasing
low (5th percentile) flow	decreasing	increasing	increasing	decreasing

3. Results

3.1. Flow regime changes

The key characteristics of a flow regime – the quantity, variability, and typical range of streamflow – exhibit globally widespread change. For all four streamflow metrics (mean, standard deviation, and high and low flows), decreasing trends are more frequent than increasing trends (Fig. 2). When looking at trends in the decreasing direction, some of the most impacted regions consist of the southwestern coast of North America, central Brazil, and the lower Mekong region – here, trends in all four metrics would suggest decreasing streamflow. Contrarily, regions including northern Amazonia and Central Europe, for example, commonly show increasing trends in all four metrics, indicating that streamflow is increasing across all facets of the flow regime.

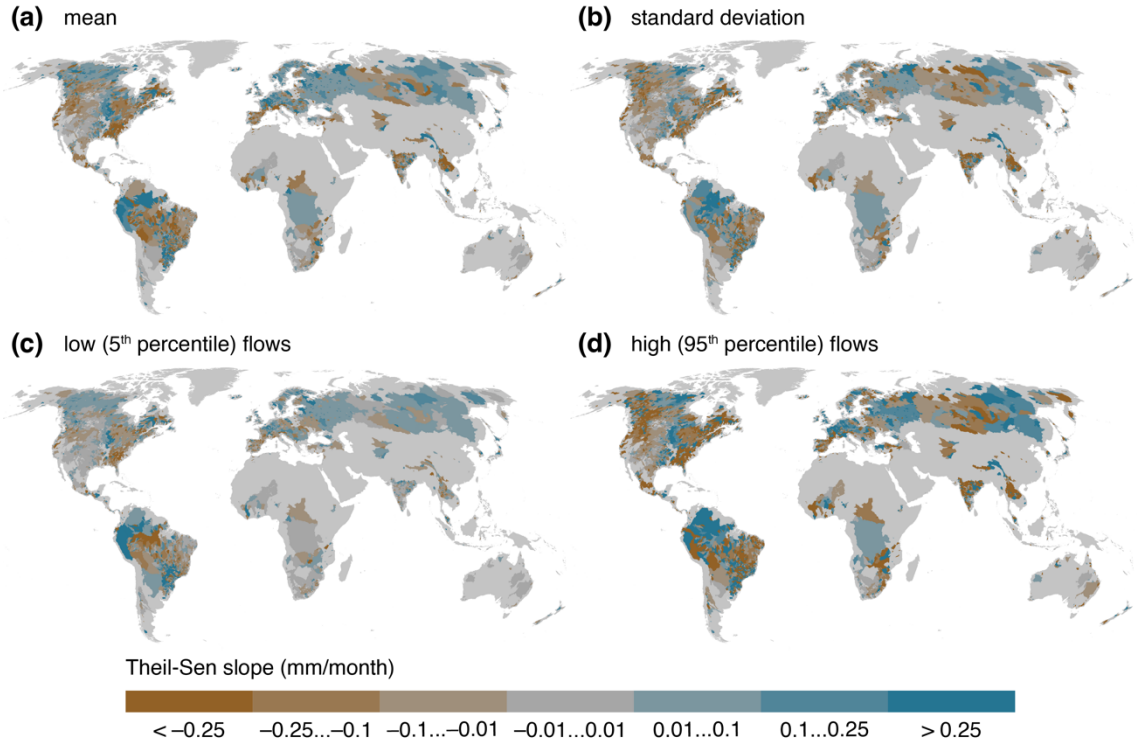

Figure 2. Linear trends in four streamflow metrics: mean (a), standard deviation (b), low (5th percentile) flows (c), and high (95th percentile) flows (d). All trends (Theil-Sen slopes) are computed based on annual metrics within the interval 1971–2010, with the sample size ranging from 10 to 40 years, depending on streamflow record length in each catchment (Fig. S1).

Catchments assigned to the four FRCs comprise 4,616 out of 5,163 (89%) of all catchments (Fig. 3). This indicates that streamflow alteration prevails throughout flow regimes, commonly in one of these four archetypal patterns. The 'shift down' and 'shrink' FRCs are more common than their opposite direction counterparts, 'shift up' and 'expand', across all catchment size groups (Fig. 3). Additionally, nearly all 'shift down' and 'shift up' catchments have, respectively, a decreasing and an increasing trend also for standard deviation (Table S1). For 'shrink' and 'expand', the fraction of this kind of parallel direction trends for the mean is not equally high (Table S1). This would suggest that decreases in streamflow quantity and variability are more common than increases, and that consistent, unidirectional shifts throughout the flow regime (either towards the drying or wetting direction) are the most common FRCs globally.

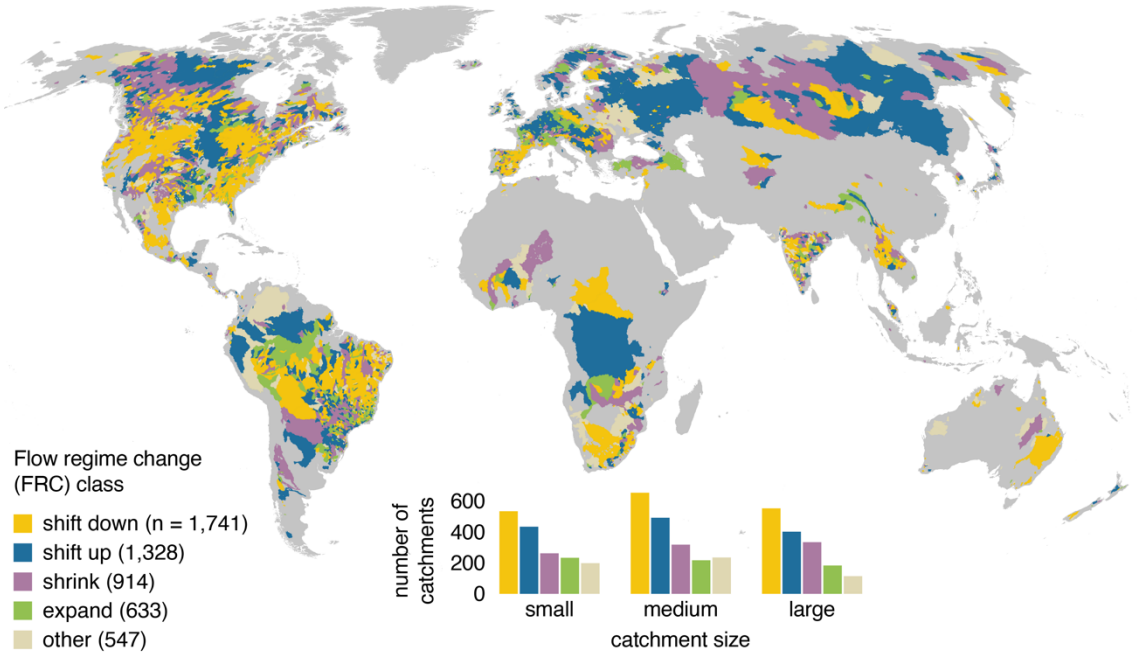

Figure 3. Assignment of flow regime change (FRC) classes for 5,163 catchments globally. The FRCs are determined by the direction of linear trends (Theil-Sen slopes) in four annual streamflow metrics (Table 1). Catchments are additionally grouped into three size groups, using a minimum catchment area of 1,000 km^2 in the small catchments group, a catchment area of 2,500 km^2 as the threshold between small and medium catchments, and a catchment area of 10,000 km^2 as the threshold between medium and large catchments.

The 'shift down' FRC is prevalent in central South America and on the eastern and western sides of North America (Fig. 3), which are regions where also the decreasing streamflow trend slopes are comparatively strong (Fig. 2). On the contrary, much of the Eurasian boreal zone and northern parts of Canada are covered by 'shift up' or 'shrink' catchments (Fig. 3). Similarly, the streamflow trend slopes there are moderate to strong (Fig. 2), although it should be noted that the geographically extensive Eurasian boreal zone is covered by relatively few large catchments (n ≈ 300). Some large basins, such as the Rhine and the Mekong, have most of their sub-catchments assigned to the same FRC with the main basin ('shift up' and 'shift down', respectively), whereas, for instance, the Tocantins and the Saskatchewan rivers have all four FRCs assigned to their sub-catchments.

3.2. Driver trends and changes

At the global scale, mean precipitation and evapotranspiration trends are moderately correlated, whereas the standard deviation trends of precipitation and evapotranspiration appear independent (Fig. 4a–d, Fig. S3). Although opposite direction trends for mean precipitation and evapotranspiration are visible at large scales in Siberia and north-western South America, for instance, trends in parallel direction for these two indirect drivers are globally prevalent (Fig. 4a–b). Mean precipitation trends (Fig. 4a) are the only case for which, among all sampled catchments, decreasing trends are more frequent than increasing trends. In contrast, for the other three climatic variables, increasing trends are more common (Fig. 4b–d).

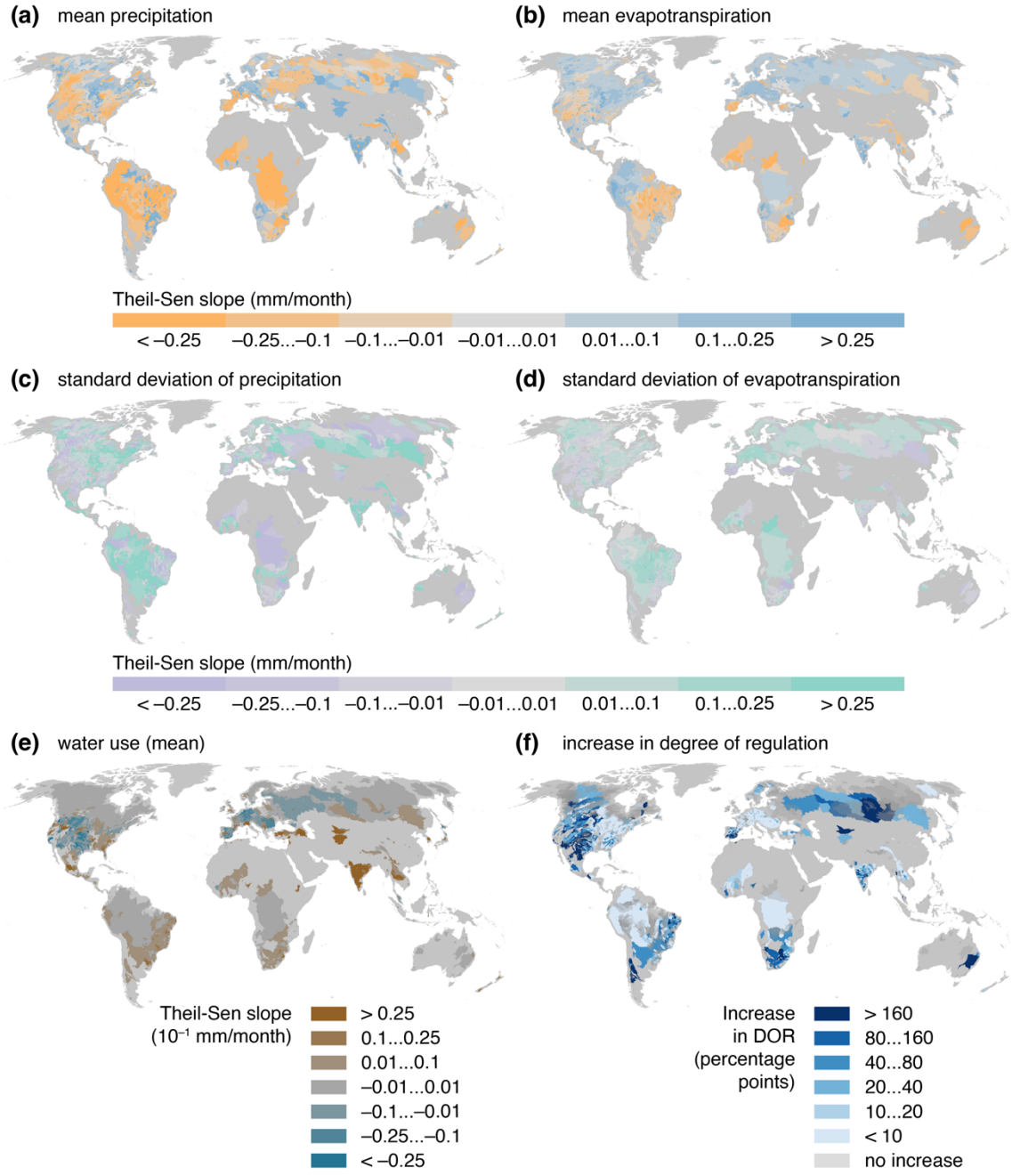

Figure 4. Trends and changes in driver variables: mean precipitation trend (a), mean evapotranspiration trend (b), trend in the standard deviation of precipitation (c), trend in the standard deviation of evapotranspiration (d), mean total water use trend (e), and increase in the degree of regulation (DOR) (f). Trends (Theil-Sen slopes) in panels (a)–(e) are computed based on annual metrics within the interval 1971–2010, with the sample size ranging from 10 to 40 years, depending on streamflow record length in each catchment (Fig. S1). For dams (f), instead of the Theil-Sen slope, change in time is assessed by absolute increase in the degree of regulation (DOR), measured in percentage points. Catchments that have not experienced an increase in DOR (being mainly sub-catchments of large basins) are overlaid on top of panel (f) with a transparent grey overlay.

Strong water use trends are concentrated in relatively small regions (Fig. 4e). On the one hand, in southern and south-eastern Asia and in the few catchments in the Caucasus and Aral Sea regions, water use trends have been strongly increasing. On the other hand, much of Europe and North America show moderate to strongly decreasing mean water use

trends. However, most regions show negligible water use trends – possibly due to their very low absolute water use. Furthermore, a total of 10,524 dams are captured within the sampled catchments, with the heaviest increases in regulation found in large catchments. Half of catchments with an area greater than 10,000 km^2 have seen an increase in DOR, whereas the same figure is 24% for catchments below this threshold. Increasing large-scale river regulation during the study period is most clearly visible in the large Siberian basins, many catchments in southern Africa and southern North America, as well as in the Murray-Darling River basin in Australia (Fig. 4f).

3.3. FRCs as indicators of likely drivers

A systematic assessment of associations between the FRC assignments (Fig. 3) and trends and changes in drivers (Fig. 4) reveals how the FRCs not only characterise changes in streamflow regimes but also allow for suggesting the most likely drivers underlying this change. This association is done here in two stages. Presuming that streamflow regimes are predominantly shaped by the amount and variability of precipitation; Fig. 5 first investigates how increasing and decreasing precipitation trends are distributed within the FRCs. Following this, Fig. 6 additionally summarises trends in evapotranspiration, water use, and changes in the degree of regulation. These two stages jointly enable a characterisation of FRCs by the most commonly occurring driver trends and changes, linking streamflow change with its external drivers.

The direction of precipitation trends mostly agrees with the direction of streamflow mean or standard deviation trend in each FRC class. For ‘shift down’ and ‘shift up’, most catchments assigned to these FRCs (70–79%) show a mean precipitation trend in decreasing and increasing direction, respectively (Fig. 5a). This could suggest that mean precipitation trends that are parallel with mean streamflow trends are associated with the ‘shift’ FRCs. For ‘expand’, most catchments similarly show an increasing trend in the standard deviation of precipitation (425 out of 612; Fig. 5b), which possibly implicates an equivalent situation, in which increasing precipitation variability may transfer to increasing streamflow variability. However, for ‘shrink’, this transfer does not appear as common, as 440 ‘shrink’ catchments show increasing trends and 433 show decreasing trends in the standard deviation of precipitation (Fig. 5b). Therefore, particularly in the case of ‘shrink’, factors beyond precipitation are likely to contribute to flow regime change.

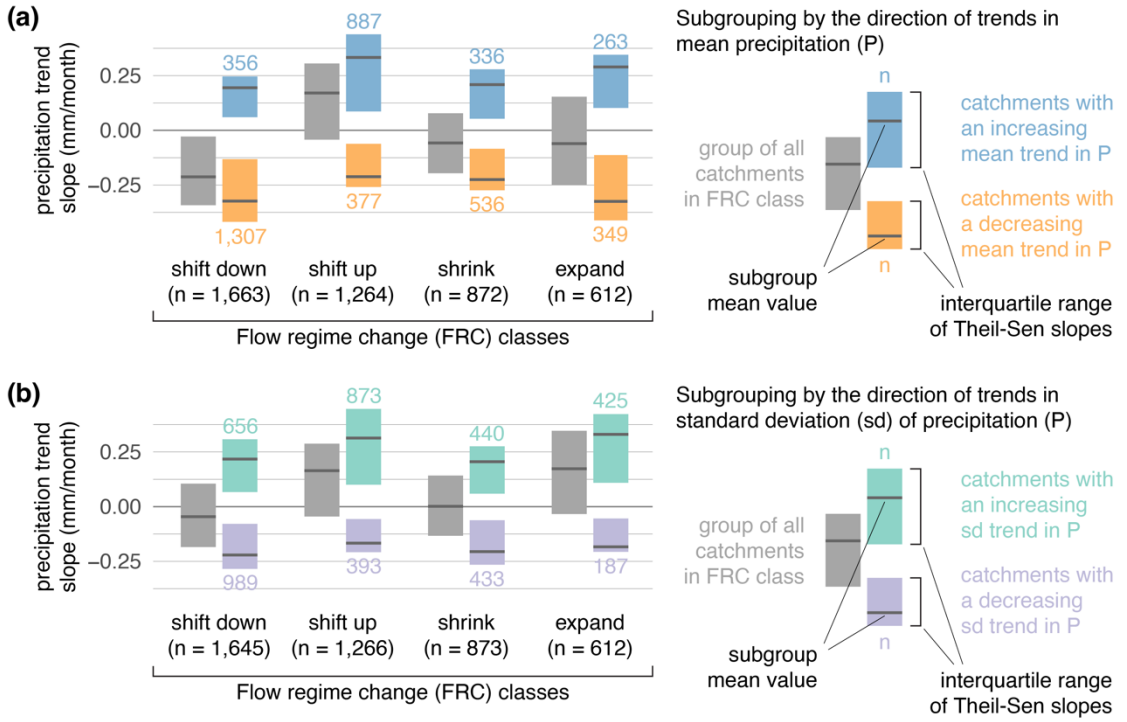

Figure 5. Grouping of catchments (n = 4,616) by linear trends in precipitation, for mean (a) and standard deviation (b). Each bar presents an interquartile range of Theil-Sen slopes in a subgroup determined by a flow regime change (FRC) class (denoted on the x-axis) and the direction of precipitation (P) trend for either mean or standard deviation (sd); subgroup mean is denoted with a horizontal line. Counts of catchments (n) in each subgroup are presented together with the interquartile ranges. Prior to drawing interquartile ranges and group means, outliers were removed from each FRC group, by excluding trend slopes with a magnitude more than two standard deviations away from the group mean.

Like how the 'expand' and 'shrink' FRCs are related with trends in precipitation variability (Fig. 5b; Fig. 6b–d), 'expand' catchments commonly show increasing trends in the standard deviation of evapotranspiration, but for 'shrink', this correspondence is not as discernible (Fig. 6e–g). Additionally, notwithstanding if the FRC describes a decreasing ('shift down') or an increasing change ('shift up') in streamflow quantity, mean evapotranspiration trends are generally weaker than precipitation trends and point to the same direction (Fig. 6b–g). This also holds for nearly all FRC subgroups consisting of catchments in which the mean precipitation trend is opposite to the mean streamflow trend; for instance, when mean precipitation trends are increasing in 'shift down' catchments (Fig. S4a–c). Therefore, in this sample, precipitation can be considered as the dominant factor among these two climate-related drivers.

Increasing water use trends are the strongest in the 'shift down' FRC (Fig. 6h–j) and additionally in the 'expand' FRC, although it should be noted that 'expand' contains the smallest number of catchments among all FRCs (Table S2). On the contrary, across all catchment size groups, water use trends in the 'shrink' FRC are relatively weak, while for the 'shift up' FRC, decreasing water use trends are common. These decreasing trends in the 'shift up' FRC become weaker towards increasing catchment sizes (Fig. 6h–j), which could suggest that decreasing water use is more likely associated with increasing streamflow quantity in small catchments but with diminishing impacts at larger scales.

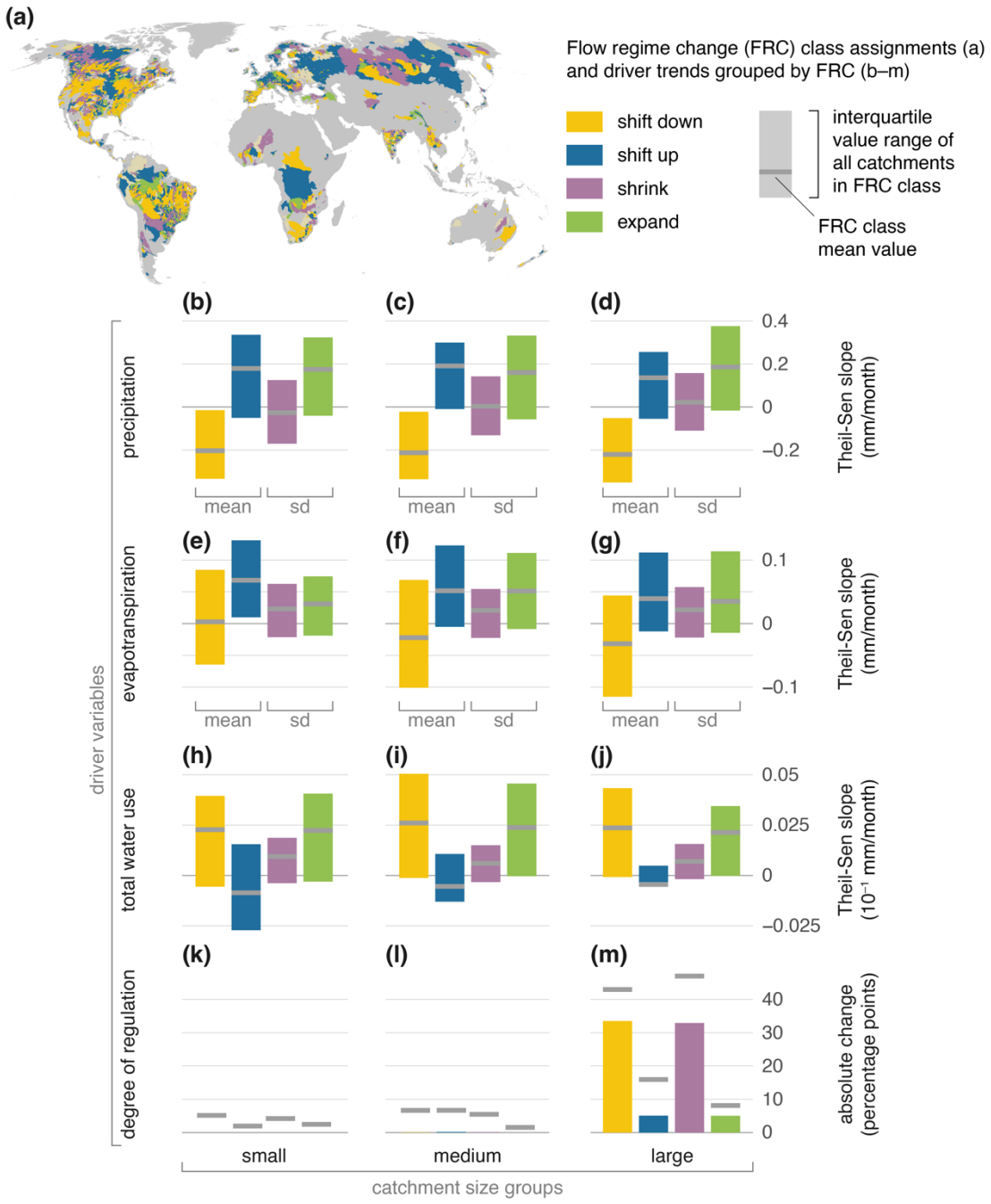

Figure 6. Flow regime change (FRC) assignments in all catchments (a) and grouping of catchments (n = 4,616) by linear trends in four driver variables: precipitation (b–d), evapotranspiration (e–g), water use (h–j), and degree of regulation (k–m). Panel (a) corresponds to Fig. 3. Each bar in panels (b)–(m) represents an interquartile range of Theil-Sen slopes in catchments assigned to an FRC class; group mean is denoted with a horizontal line. For precipitation and evapotranspiration, the FRC groups 'shift down' and 'shift up' display trends in mean, whereas the FRC groups 'shrink' and 'expand' display trends in standard deviation (sd). For water use, all FRC groups display trends in mean. Catchments are additionally grouped into three size groups, using a minimum catchment area of 1,000 km^2 in the small catchments group (b, e, h, k), a catchment area of 2,500 km^2 as the threshold between small and medium catchments (c, f, i, l), and a catchment area of 10,000 km^2 as the threshold between medium and large catchments (d, g, j, m). Prior to drawing interquartile ranges and group means, outliers were removed from each FRC group, by excluding trend slopes with a magnitude more than two standard deviations away from the group mean.

Increases in DOR are heavily concentrated in large catchments in the 'shift down' and 'shrink' FRCs (Fig. 6k–m). Although some damming occurs across all catchment size

groups and FRCs – evidenced by the group means in Fig. 6k–m rising above zero – large catchments are by far the most affected. A peculiar example of damming is seen in the 'shift down' FRC subgroup where precipitation trends are increasing; here, the mean increase in DOR reaches more than 60 percentage points and is notably larger than in any other subgroup (Fig. S4i). Though this group consists of relatively few catchments (n = 107; Table S2), the divergence may suggest cases in which large-scale flow regulation combined with increased water use (Fig. S4f) potentially offset the increasing water availability trend, eventually resulting in decreased streamflow.

To summarise, the role of indirect drivers – precipitation and evapotranspiration – is strong in all FRCs except for 'shrink', which appears primarily associated with increasing flow regulation. The 'shift down' FRC is additionally associated with strongly increasing trends in water use, and thus heavily affected by both direct and indirect drivers. The 'expand' and 'shift up' FRCs likely associate the strongest with indirect drivers, while some evidence exists for water use possibly reshaping flow regimes in the 'expand' FRC and replenishing streamflow in the 'shift up' FRC.

As the FRCs are characterised not only by streamflow trends but also by driver trends (Fig. 5–6), the FRC map (Fig. 3, Fig. 6a) also serves as a map of the likely drivers of streamflow change. The systematic association analysis supports general patterns of, for example, 'shift down' catchments often aligning with the most intensive water use regions and 'shrink' catchments with the heaviest flow regulation (Fig. 3–4). Although the globally most frequent associations do not necessarily hold in all individual catchments, these distinct characterisations of the four FRCs can suggest relatively generalised relations between streamflow change and its drivers.

4. Discussion

The FRC assignments (Fig. 3) correspond well with independent estimates of streamflow change. The spatially extensive FRCs 'shift down', 'shift up' and 'shrink' largely agree with estimates of increased frequency of exceptionally dry and wet conditions, analogous to alteration in low and high flows (Porkka et al., 2024). This is the case, especially in South and North America and Europe, where our catchment sampling density is the highest. Similarly, the FRCs coincide with recent trends in water availability in South America, but at the same time, discrepancies are seen in the large Mississippi River basin where the 'shift down' FRC is prevalent, notwithstanding an increasing trend in water availability (Zhang et al., 2023). This may be due to high water use (Huang et al., 2018) and flow regulation (Grill et al., 2019) in the region, which both associate with the 'shift down' FRC.

In our catchment sample, precipitation outweighs evapotranspiration as the more dominant driver of change in water availability, which agrees with Zhang et al. (2023), who find similar dominance across regions that contain most of our catchments. Furthermore, climate change contributes to decreasing streamflow across South and North America and the Mediterranean, and to increasing streamflow in Northern Europe (Gudmundsson et al., 2021), which often show instances of the 'shift down' and 'shift up' FRCs, respectively. Direct drivers being especially relevant for the 'shrink' and 'shift

down' FRCs and showing moderate association with the 'expand' FRC additionally agrees with Yang et al. (2021) and Pastor et al. (2022), who find that streamflow changes are more likely in the strong presence of direct human drivers.

In agreement with comparable studies (Gudmundsson et al., 2021; Pastor et al., 2022; Porkka et al., 2024; Yang et al., 2021; Zhang et al., 2023), we find that associations between streamflow change and its drivers vary spatially. Therefore, the main limitation of this study is that the globally most frequent associations do not necessarily implicate causal relationships at the scale of individual catchments. Additionally, although we characterise the FRCs by driver trends that presumably propagate to streamflow alteration, we are unable to robustly assess the absolute contributions of the different drivers (for example, how many units does streamflow change, given a unit change in precipitation). Moreover, our study lacks explicit representation of groundwater that has a considerable impact on streamflow and is subject to manifold human pressures (Kuang et al., 2024).

Notwithstanding the above outlined limitations of this study, our proposed FRCs allow for shaping generic associations between streamflow change and its drivers. In future research, following recent developments of releasing observed streamflow data in structured collections (Kratzert et al., 2023) and evolving future projections (Frieler et al., 2024) can develop and further validate our main results across scales. Ideally with even more comprehensive catchment samples and additional drivers, future studies can increasingly add to understanding the complex dynamics of streamflow change. Advancing this knowledge is essential for evaluating the most impactful and meaningful measures for mitigating adverse impacts stemming from streamflow change.

5. Conclusion

Here, we have shown how the formation of four archetypal flow regime change (FRC) classes can provide a straightforward way to associate streamflow alteration with its drivers. Nearly all catchments (89%) in our sample are assigned to one of the four FRC classes, which also appear associated with trends in the key drivers of streamflow alteration. We find that indirect drivers, including precipitation and evapotranspiration, are strongly related with all FRCs except for 'shrink', which describes decreasing streamflow variability and is strongly linked with increasing flow regulation. Increasing water use and decreasing trends in water availability are frequently associated with decreasing streamflow, as described by the 'shift down' FRC. The 'shift up' and 'expand' FRCs that describe increasing quantity and variability of streamflow, respectively, are weaker coupled with direct human drivers, although some moderate associations exist. These observation-based outcomes substantiate existing modelling studies both on the extent and drivers of streamflow change. Our results highlight the globally most prevalent relations between streamflow regime alterations and their drivers, which offers action points for mitigating the adverse impacts of streamflow change. This can further support and advance studies aiming to decrease the manifold human pressures on the freshwater cycle.

References

Adler, R.F., Gu, G., Sapiano, M., Wang, J.-J., Huffman, G.J., 2017. Global Precipitation: Means, Variations and Trends During the Satellite Era (1979–2014). Surv. Geophys. 38, 679–699. https://doi.org/10.1007/s10712-017-9416-4

Baston, D., 2022. exactextractr: Fast Extraction from Raster Datasets using Polygons. R package version 0.9.1, https://cran.r-project.org/web/packages/exactextractr/index.html

Best, J., 2019. Anthropogenic stresses on the world's big rivers. Nat. Geosci. 12, 7–21. https://doi.org/10.1038/s41561-018-0262-x

Chagas, V.B.P., Chaffe, P.L.B., Blöschl, G., 2022. Climate and land management accelerate the Brazilian water cycle. Nat. Commun. 13, 5136. https://doi.org/10.1038/s41467-022-32580-x

Dennedy-Frank, P.J., Gorelick, S.M., 2019. Insights from watershed simulations around the world: Watershed service-based restoration does not significantly enhance streamflow. Glob. Environ. Change 58, 101938. https://doi.org/10.1016/j.gloenvcha.2019.101938

Do, H.X., Gudmundsson, L., Leonard, M., Westra, S., 2018. The Global Streamflow Indices and Metadata Archive (GSIM) – Part 1: The production of a daily streamflow archive and metadata. Earth Syst. Sci. Data 10, 765–785. https://doi.org/10.5194/essd-10-765-2018

Frieler, K., Volkholz, J., Lange, S., Schewe, J., Mengel, M., del Rocío Rivas López, M., Otto, C., Reyer, C.P.O., Karger, D.N., Malle, J.T., Treu, S., Menz, C., Blanchard, J.L., Harrison, C.S., Petrik, C.M., Eddy, T.D., Ortega-Cisneros, K., Novaglio, C., Rousseau, Y., Watson, R.A., Stock, C., Liu, X., Heneghan, R., Tittensor, D., Maury, O., Büchner, M., Vogt, T., Wang, T., Sun, F., Sauer, I.J., Koch, J., Vanderkelen, I., Jägermeyr, J., Müller, C., Rabin, S., Klar, J., Vega del Valle, I.D., Lasslop, G., Chadburn, S., Burke, E., Gallego-Sala, A., Smith, N., Chang, J., Hantson, S., Burton, C., Gädeke, A., Li, F., Gosling, S.N., Müller Schmied, H., Hattermann, F., Wang, J., Yao, F., Hickler, T., Marcé, R., Pierson, D., Thiery, W., Mercado-Bettín, D., Ladwig, R., Ayala-Zamora, A.I., Forrest, M., Bechtold, M., 2024. Scenario setup and forcing data for impact model evaluation and impact attribution within the third round of the Inter-Sectoral Model Intercomparison Project (ISIMIP3a). Geosci. Model Dev. 17, 1–51. https://doi.org/10.5194/gmd-17-1-2024

Gleeson, T., Wang-Erlandsson, L., Porkka, M., Zipper, S.C., Jaramillo, F., Gerten, D., Fetzer, I., Cornell, S.E., Piemontese, L., Gordon, L.J., Rockström, J., Oki, T., Sivapalan, M., Wada, Y., Brauman, K.A., Flörke, M., Bierkens, M.F.P., Lehner, B., Keys, P., Kummu, M., Wagener, T., Dadson, S., Troy, T.J., Steffen, W., Falkenmark, M., Famiglietti, J.S., 2020. Illuminating water cycle modifications and Earth system resilience in the Anthropocene. Water Resour. Res. 56, e2019WR024957. https://doi.org/10.1029/2019WR024957

GRDC, 2023. BfG - The GRDC [WWW Document]. URL https://portal.grdc.bafg.de/applications/public.html?publicuser=PublicUser#dataDownload/StationCatalogue (accessed November 14th, 2023).

Grill, G., Lehner, B., Thieme, M., Geenen, B., Tickner, D., Antonelli, F., Babu, S., Borrelli, P., Cheng, L., Crochetiere, H., Ehalt Macedo, H., Filgueiras, R., Goichot, M., Higgins, J., Hogan, Z., Lip, B., McClain, M.E., Meng, J., Mulligan, M., Nilsson, C., Olden, J.D., Opperman, J.J., Petry, P., Reidy Liermann, C., Sáenz, L., Salinas-Rodríguez, S., Schelle, P., Schmitt, R.J.P., Snider, J., Tan, F., Tockner, K., Valdujo, P.H., van Soesbergen, A., Zarfl, C., 2019. Mapping the world's free-flowing rivers. Nature 569, 215–221. https://doi.org/10.1038/s41586-019-1111-9

Gudmundsson, L., Boulange, J., Do, H.X., Gosling, S.N., Grillakis, M.G., Koutroulis, A.G., Leonard, M., Liu, J., Schmied, H.M., Papadimitriou, L., Pokhrel, Y., Seneviratne, S.I., Satoh, Y., Thiery, W., Westra, S., Zhang, X., Zhao, F., 2021. Globally observed trends in mean and extreme river flow attributed to climate change. Science 371, 1159–1162. https://doi.org/10.1126/science.aba3996

Gudmundsson, L., Do, H.X., Leonard, M., Westra, S., 2018. The Global Streamflow Indices and Metadata Archive (GSIM) – Part 2: Quality control, time-series indices and homogeneity assessment. Earth Syst. Sci. Data 10, 787–804. https://doi.org/10.5194/essd-10-787-2018

Horton, A.J., Nygren, A., Diaz-Perera, M.A., Kummu, M., 2021. Flood severity along the Usumacinta River, Mexico: Identifying the anthropogenic signature of tropical forest conversion. J. Hydrol. X 10, 100072. https://doi.org/10.1016/j.hydroa.2020.100072

Huang, Z., Hejazi, M., Li, X., Tang, Q., Vernon, C., Leng, G., Liu, Y., Döll, P., Eisner, S., Gerten, D., Hanasaki, N., Wada, Y., 2018. Reconstruction of global gridded monthly sectoral water withdrawals for 1971–2010 and analysis of their spatiotemporal patterns. Hydrol. Earth Syst. Sci. 22, 2117–2133. https://doi.org/10.5194/hess-22-2117-2018

Hurtado, S.I., 2020. RobustLinearReg: Robust Linear Regressions. R package version 1.2.0, https://cran.r-project.org/web/packages/RobustLinearReg/index.html

Kåresdotter, E., Destouni, G., Ghajarnia, N., Lammers, R.B., Kalantari, Z., 2022. Distinguishing Direct Human-Driven Effects on the Global Terrestrial Water Cycle. Earths Future 10, e2022EF002848. https://doi.org/10.1029/2022EF002848

Kratzert, F., Nearing, G., Addor, N., Erickson, T., Gauch, M., Gilon, O., Gudmundsson, L., Hassidim, A., Klotz, D., Nevo, S., Shalev, G., Matias, Y., 2023. Caravan - A global community dataset for large-sample hydrology. Sci. Data 10, 61. https://doi.org/10.1038/s41597-023-01975-w

Kuang, X., Liu, J., Scanlon, B.R., Jiao, J.J., Jasechko, S., Lancia, M., Biskaborn, B.K., Wada, Y., Li, H., Zeng, Z., Guo, Z., Yao, Y., Gleeson, T., Nicot, J.-P., Luo, X., Zou, Y., Zheng, C., 2024. The changing nature of groundwater in the global water cycle. Science 383, eadf0630. https://doi.org/10.1126/science.adf0630

Levy, M.C., Lopes, A.V., Cohn, A., Larsen, L.G., Thompson, S.E., 2018. Land Use Change Increases Streamflow Across the Arc of Deforestation in Brazil. Geophys. Res. Lett. 45, 3520–3530. https://doi.org/10.1002/2017GL076526

Muñoz-Sabater, J., Dutra, E., Agustí-Panareda, A., Albergel, C., Arduini, G., Balsamo, G., Boussetta, S., Choulga, M., Harrigan, S., Hersbach, H., Martens, B., Miralles, D.G., Piles, M., Rodríguez-Fernández, N.J., Zsoter, E., Buontempo, C., Thépaut, J.-N., 2021. ERA5-Land: a state-of-the-art global reanalysis dataset for land applications. Earth Syst. Sci. Data 13, 4349–4383. https://doi.org/10.5194/essd-13-4349-2021

Nilsson, C., Reidy, C.A., Dynesius, M., Revenga, C., 2005. Fragmentation and Flow Regulation of the World's Large River Systems. Science 308, 405–408. https://doi.org/10.1126/science.1107887

Pastor, A.V., Biemans, H., Franssen, W., Gerten, D., Hoff, H., Ludwig, F., Kabat, P., 2022. Understanding the transgression of global and regional freshwater planetary boundaries. Philos. Trans. R. Soc. Math. Phys. Eng. Sci. 380, 20210294. https://doi.org/10.1098/rsta.2021.0294

Poff, N.L., Olden, J.D., Merritt, D.M., Pepin, D.M., 2007. Homogenization of regional river dynamics by dams and global biodiversity implications. Proc. Natl. Acad. Sci. 104, 5732–5737. https://doi.org/10.1073/pnas.0609812104

Porkka, M., Virkki, V., Wang-Erlandsson, L., Gerten, D., Gleeson, T., Mohan, C., Fetzer, I., Jaramillo, F., Staal, A., te Wierik, S., Tobian, A., van der Ent, R., Döll, P., Flörke, M., Gosling, S.N., Hanasaki, N., Satoh, Y., Müller Schmied, H., Wanders, N., Famiglietti, J.S., Rockström, J., Kummu, M., 2024. Notable shifts beyond pre-industrial streamflow and soil moisture conditions transgress the planetary boundary for freshwater change. Nat. Water 2, 262–273. https://doi.org/10.1038/s44221-024-00208-7

Richardson, K., Steffen, W., Lucht, W., Bendtsen, J., Cornell, S.E., Donges, J.F., Drüke, M., Fetzer, I., Bala, G., von Bloh, W., Feulner, G., Fiedler, S., Gerten, D., Gleeson, T., Hofmann, M., Huiskamp, W., Kummu, M., Mohan, C., Nogués-Bravo, D., Petri, S., Porkka, M., Rahmstorf, S., Schaphoff, S., Thonicke, K., Tobian, A., Virkki, V., Wang-Erlandsson, L., Weber, L., Rockström, J., 2023. Earth beyond six of nine planetary boundaries. Sci. Adv. 9, eadh2458. https://doi.org/10.1126/sciadv.adh2458

Telteu, C.-E., Müller Schmied, H., Thiery, W., Leng, G., Burek, P., Liu, X., Boulange, J.E.S., Andersen, L.S., Grillakis, M., Gosling, S.N., Satoh, Y., Rakovec, O., Stacke, T., Chang, J., Wanders, N., Shah, H.L., Trautmann, T., Mao, G., Hanasaki, N., Koutroulis, A., Pokhrel, Y., Samaniego, L., Wada, Y., Mishra, V., Liu, J., Döll, P., Zhao, F., Gädeke, A., Rabin, S.S., Herz, F., 2021. Understanding each other's models: an introduction and a standard representation of 16 global water models to support intercomparison, improvement, and communication. Geosci. Model Dev. 14, 3843–3878. https://doi.org/10.5194/gmd-14-3843-2021

Theeuwen, J.J.E., Staal, A., Tuinenburg, O.A., Hamelers, B.V.M., Dekker, S.C., 2023. Local moisture recycling across the globe. Hydrol. Earth Syst. Sci. 27, 1457–1476. https://doi.org/10.5194/hess-27-1457-2023

Veldkamp, T.I.E., Zhao, F., Ward, P.J., Moel, H. de, Aerts, J.C.J.H., Schmied, H.M., Portmann, F.T., Masaki, Y., Pokhrel, Y., Liu, X., Satoh, Y., Gerten, D., Gosling, S.N., Zaherpour, J., Wada, Y., 2018. Human impact parameterizations in global hydrological models improve estimates of monthly discharges and hydrological extremes: a multi-model validation study. Environ. Res. Lett. 13, 055008. https://doi.org/10.1088/1748-9326/aab96f

Virkki, V., Alanärä, E., Porkka, M., Ahopelto, L., Gleeson, T., Mohan, C., Wang-Erlandsson, L., Flörke, M., Gerten, D., Gosling, S.N., Hanasaki, N., Müller Schmied, H., Wanders, N., Kummu, M., 2022. Globally widespread and increasing violations of environmental flow envelopes. Hydrol. Earth Syst. Sci. 26, 3315–3336. https://doi.org/10.5194/hess-26-3315-2022

Wada, Y., Bierkens, M.F.P., 2014. Sustainability of global water use: past reconstruction and future projections. Environ. Res. Lett. 9, 104003. https://doi.org/10.1088/1748-9326/9/10/104003

Wang, J., Walter, B.A., Yao, F., Song, C., Ding, M., Maroof, A.S., Zhu, J., Fan, C., McAlister, J.M., Sikder, S., Sheng, Y., Allen, G.H., Crétaux, J.-F., Wada, Y., 2022. GeoDAR: georeferenced global dams and reservoirs dataset for bridging attributes and geolocations. Earth Syst. Sci. Data 14, 1869–1899. https://doi.org/10.5194/essd-14-1869-2022

Wang-Erlandsson, L., Fetzer, I., Keys, P.W., van der Ent, R.J., Savenije, H.H.G., Gordon, L.J., 2018. Remote land use impacts on river flows through atmospheric teleconnections. Hydrol. Earth Syst. Sci. 22, 4311–4328. https://doi.org/10.5194/hess-22-4311-2018

Yang, Y., Roderick, M.L., Yang, D., Wang, Z., Ruan, F., McVicar, T.R., Zhang, S., Beck, H.E., 2021. Streamflow stationarity in a changing world. Environ. Res. Lett. 16, 064096. https://doi.org/10.1088/1748-9326/ac08c1

Zhang, Y., Li, C., Chiew, F.H.S., Post, D.A., Zhang, X., Ma, N., Tian, J., Kong, D., Leung, L.R., Yu, Q., Shi, J., Liu, C., 2023. Southern Hemisphere dominates recent decline in global water availability. Science 382, 579–584. https://doi.org/10.1126/science.adh0716

Acknowledgements

Parts of this work were conducted in the Young Scientists Summer Program 2023, hosted by the International Institute for Applied Systems Analysis (IIASA) in Laxenburg, Austria.

This work was funded by the Aalto University School of Engineering Doctoral Programme (V.V.), European Research Council (ERC) grants number 819202 (V.V., M.P., M.K.) and 101118083 (M.P.), the Research Council of Finland grant WATVUL; grant number 317320 (M.K.), and the Research Council of Finland's Flagship Programme under the project Digital Waters; grant number 359248 (M.K.).

Author contributions

V.V., R.K.S., M.S. and M.K. conceptualised the study. V.V. gathered the data, conducted the analysis, and produced the outputs shown in the study with help from R.K.S., M.S., J.L.-R., and M.K. V.V. wrote the manuscript with input from all authors.

Data availability statement

Output data supporting the findings of this study will be deposited in a public repository (https://doi.org/10.5281/zenodo.11102423) and released upon publication, given restrictions on redistributing proprietary source data, namely WRD dam attributes, which were acquired with an Aalto University licence.

Code used in producing the results shown in this study will be deposited in a public database and released upon publication**.**

Competing interests

Authors declare that they have no competing interests.

Supplementary materials

Supplementary materials attached to this manuscript contain Figures S1–S4 and Tables S1–S2.

This is a non-peer reviewed preprint submitted to EarthArXiv.
The manuscript has been submitted for review in Environmental Research Letters.

Supplementary material for

Archetypal flow regime change classes as signatures of anthropogenic drivers of global streamflow alterations

Vili Virkki[1,2,*], Reetik Kumar Sahu[2], Mikhail Smilovic[2], Josias Láng-Ritter[1,3], Miina Porkka[1,4], Matti Kummu[1,*]

[1] Water and Development Research Group, Aalto University; Espoo, Finland
[2] Water Security Research Group, Biodiversity and Natural Resources Program, International Institute for Applied Systems Analysis (IIASA); Laxenburg, A-2361, Austria
[3] GIScience for Sustainability Transitions Lab, Aalto University; Espoo, Finland
[4] Department of Environmental and Biological Sciences, University of Eastern Finland; Joensuu, Finland

* Corresponding authors. Email: vili.virkki@aalto.fi, matti.kummu@aalto.fi

This supplementary material contains

Figures S1–S4
Tables S1–S2

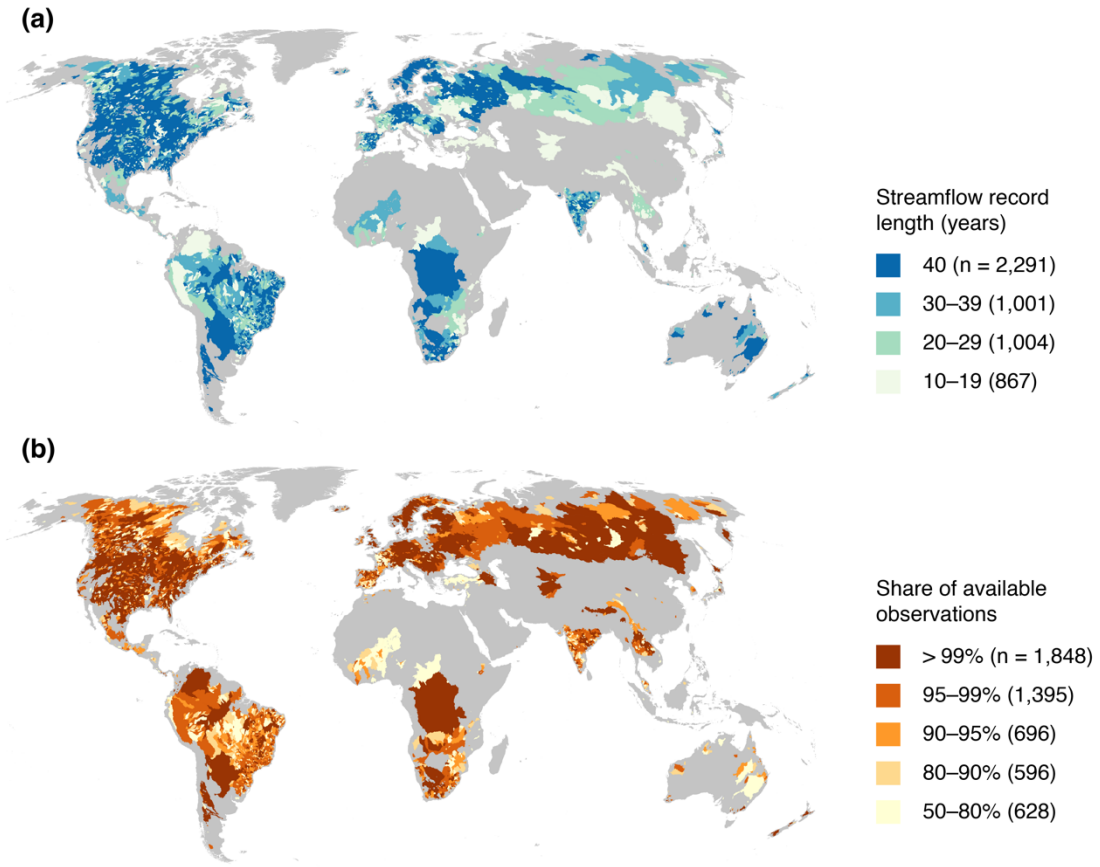

Figure S1. Catchment sample characteristics: streamflow record length (a) and the share of available observations (b). Streamflow record length refers to the maximum number of years (last year – first year + 1) covered by observations in an individual catchment (streamflow gauge). Share of available observations denotes the fraction of months that have available observations, out of all months between the first and last month of record.

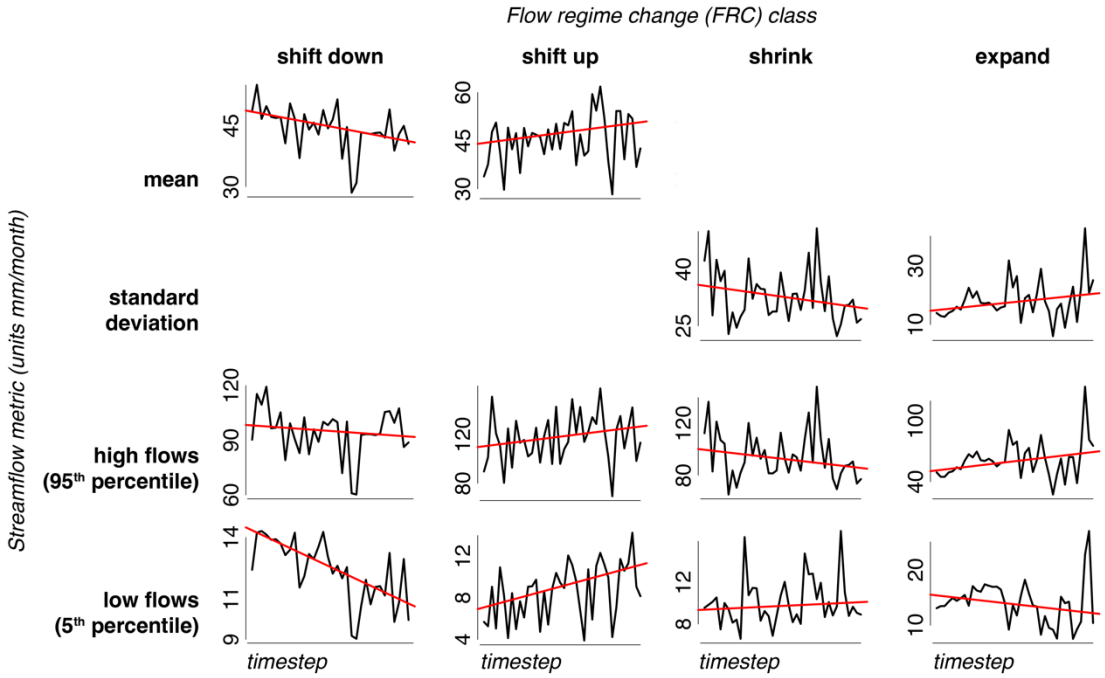

Figure S2. Case examples of assigning flow regime change (FRC) classes in four individual catchments (plot grid columns). For each catchment, four annual streamflow metrics (plot grid rows) are computed, and Theil-Sen slopes (red solid line) are estimated based on these annual metrics (black solid line). Catchments are assigned to an FRC class (plot grid column headers) based on the combination of the four Theil-Sen slopes (Table 1).

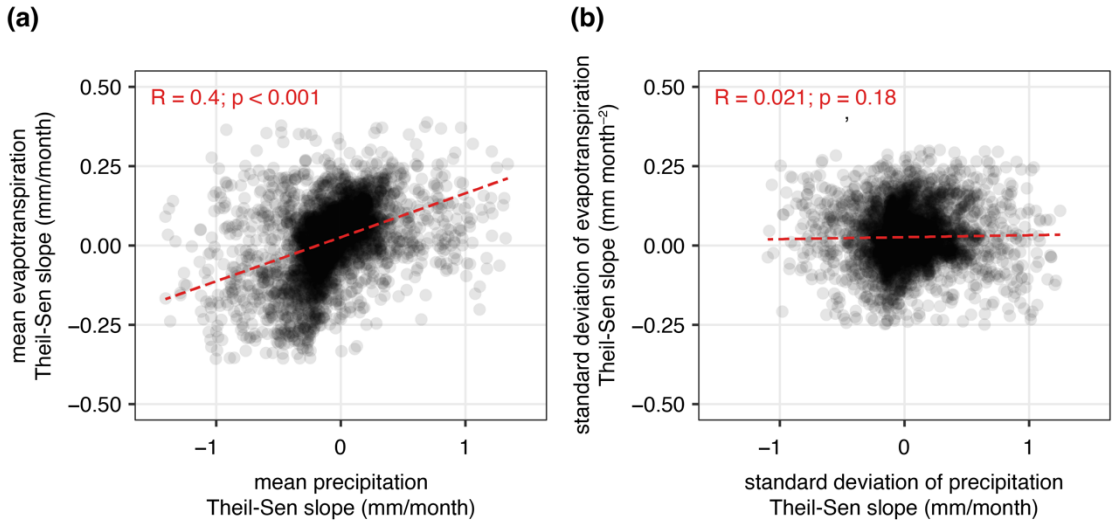

Figure S3. Correlation between precipitation and evapotranspiration trends, for trends in mean (a) and standard deviation (b). Each dot represents an individual catchment. Pearson's correlation coefficient (R) is provided together with a best-fit ordinary least squares regression line (dashed red line); regression significance (p value) is tested at a 95% confidence level. Before the correlation analysis, outliers were removed by excluding trend slopes with magnitude more than two standard deviations away from the mean trend slope.

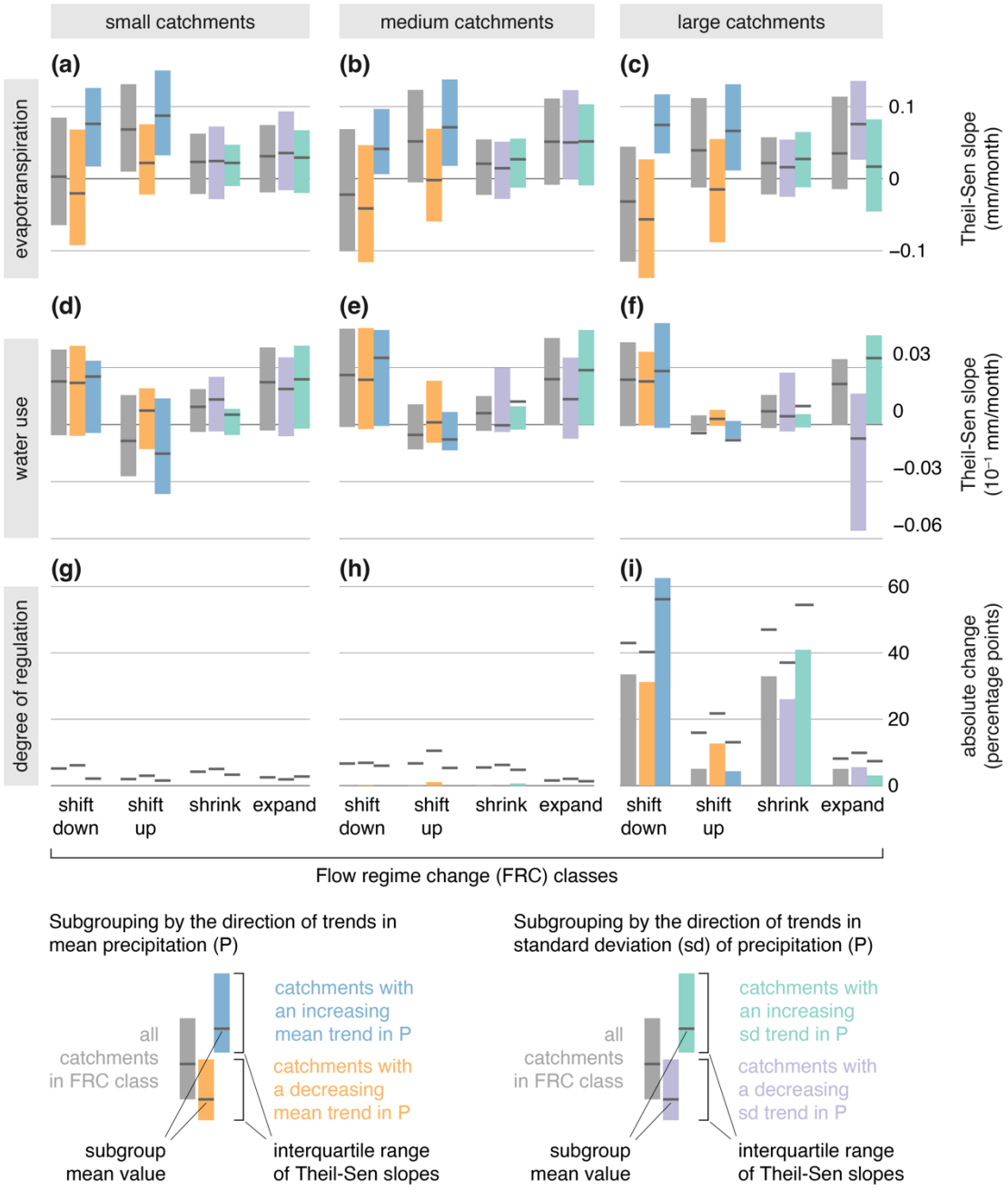

Figure S4. Grouping of catchments (n = 4,616) by linear trends in three driver variables: evapotranspiration (a–c), water use (d–f), and degree of regulation (g–i). Subgroups within each flow regime change (FRC) class (denoted on the x-axis) are created based on whether precipitation trends are increasing or decreasing. The coloured bars delimit the interquartile range of Theil-Sen slopes in each subgroup; subgroup mean is denoted with a horizontal line. For evapotranspiration (a–c), the FRC groups 'shift down' and 'shift up' display trends in mean, whereas the FRC groups 'shrink' and 'expand' display trends in standard deviation. Catchments are additionally separated by size, using a minimum catchment area of 1,000 km^2 in the small catchments group (a, d, g), a catchment area of 2,500 km^2 as the threshold between small and medium catchments (b, e, h), and a catchment area of 10,000 km^2 as the threshold between medium and large catchments (c, f, i). Prior to drawing interquartile ranges and group means, outliers were removed from each FRC–area class group, by excluding trend slopes with magnitude more than two standard deviations away from the group mean.

Table S1. Counts of streamflow trends (Theil-Sen slope directions) in the four main flow regime change (FRC) classes. According to the FRC assignment rules (Table 1), three out of four conditions for each streamflow metric and FRC class are fixed (denoted by 'all' in this Table). The 'unconstrained' condition (Table 1) may be increasing or decreasing (Theil-Sen slope can be either negative or positive), or in few cases zero. For 'shift down' and 'shift up', the unconstrained condition is the trend in the standard deviation of streamflow, whereas for 'shrink' and 'expand', the unconstrained condition is the trend in mean streamflow.

Streamflow metric	*Flow regime change (FRC) class*			
	'shift down'	**'shift up'**	**'shrink'**	**'expand'**
mean				
increasing	0	1,328 (all)	330	419
decreasing	1,741 (all)	0	584	212
zero slope	0	0	0	2
standard deviation				
increasing	156	1,154	0	633 (all)
decreasing	1,583	174	914 (all)	0
zero slope	2	0	0	0
high (95th percentile) flow				
increasing	0	1,328 (all)	0	633 (all)
decreasing	1,741 (all)	0	914 (all)	0
zero slope	0	0	0	0
low (5th percentile) flow				
increasing	0	1,328 (all)	914 (all)	0
decreasing	1,741 (all)	0	0	633 (all)
zero slope	0	0	0	0

Table S2. Sample sizes for subgroups presented in Fig. S4. Subgroups are created by catchment area group, flow regime change (FRC) class, and the direction of precipitation trend (all trends, increasing trends only, or decreasing trends only). For 'shift down' and 'shift up', the precipitation trend is the trend in mean, whereas for 'shrink' and 'expand', the precipitation trend is the trend in standard deviation.

Subgrouping by			**Number of catchments in subgroup for**		
catchment area group	*FRC class*	*precipitation trend*	*evapotran-spiration*	*water use*	*degree of regulation*
small	shift down	all	508	518	521
small	shift down	decreasing	386	401	396
small	shift down	increasing	122	117	125
small	shift up	all	410	417	424
small	shift up	decreasing	120	123	123
small	shift up	increasing	290	294	301
small	shrink	all	252	254	254
small	shrink	decreasing	129	132	133
small	shrink	increasing	123	122	121
small	expand	all	224	226	227
small	expand	decreasing	67	66	70
small	expand	increasing	157	160	157
medium	shift down	all	624	626	633
medium	shift down	decreasing	479	491	485
medium	shift down	increasing	145	135	148
medium	shift up	all	468	475	486
medium	shift up	decreasing	125	127	128
medium	shift up	increasing	343	348	358
medium	shrink	all	301	309	301
medium	shrink	decreasing	148	153	145
medium	shrink	increasing	153	156	156
medium	expand	all	206	212	209
medium	expand	decreasing	65	67	64
medium	expand	increasing	141	145	145
large	shift down	all	525	526	552
large	shift down	decreasing	426	438	445
large	shift down	increasing	99	88	107
large	shift up	all	386	392	398
large	shift up	decreasing	128	131	132
large	shift up	increasing	258	261	266
large	shrink	all	318	311	330
large	shrink	decreasing	156	150	158
large	shrink	increasing	162	161	172
large	expand	all	177	174	177
large	expand	decreasing	55	56	54
large	expand	increasing	122	118	123